J. Fluid Mech. (1977), *vol.* 81, *part* 1, *pp.* 85–105
Printed in Great Britain

The added mass of two-dimensional cylinders heaving in water of finite depth

By KWANG JUNE BAI

David W. Taylor Naval Ship Research and Development Center,
Bethesda, Maryland 20084

(Received 19 April 1976)

This paper presents numerical results for the added-mass and damping coefficients of semi-submerged two-dimensional heaving cylinders in water of finite depth. A simple proof is given which shows that the added mass is bounded for all frequencies in water of finite depth. The limits of the added-mass and damping coefficients are studied as the frequency tends to zero and to infinity. A new formulation valid in the low-frequency limit is constructed by using a perturbation expansion in the wave-number parameter. For the limiting cases, dual extremum principles are used, which consist of two variational principles: a minimum principle for a functional and a maximum principle for a different but related functional. These two functionals are used to obtain lower and upper bounds on the added mass in the limiting cases. However, the functionals constructed (Bai & Yeung 1974) for the general frequency range (excluding the limiting cases) have neither a minimum nor a maximum. In this case, the approximate solution cannot be proved to be bounded either below or above by the true solution. To illustrate these methods, the added-mass and damping coefficients are computed for a circular cylinder oscillating in water of several different depths. Results are also presented for rectangular cylinders with three different beam–draft ratios at several water depths.

1. Introduction

Small oscillatory motions of a two-dimensional cylinder in an inviscid incompressible fluid of finite depth with a free surface are described by a boundary-value problem governed by Laplace's equation with a Neumann condition on the cylinder, a mixed-type boundary condition on the free surface, a homogeneous Neumann condition on the bottom and an appropriate radiation condition at infinity. Yu & Ursell (1961) considered the above problem for a semi-submerged circular cylinder in water of finite depth and found the added-mass and damping coefficients. Lebreton & Margnac (1966) computed the added-mass and damping coefficients for rectangular cylinders on the free surface of water of finite depth. Kim (1967) computed the added-mass and damping coefficients for circular and Lewis-form (nearly rectangular) cylinders in water of finite depth. Keil (1974) extended Grim's method of multipole expansions to bodies in water of finite depth and computed the heave added-mass and damping coefficients of circular and Lewis-form (nearly rectangular) sections. Bai & Yeung (1974) also made computations of the heave added-mass and damping coefficients of both circular and rectangular sections in water of finite depth. The computa-

tions of Bai & Yeung agree with the results of Lebreton & Margnac and Keil but disagree with the other two earlier computations, which moreover differ among themselves. The disagreement is most striking in the small-frequency range: the added-mass coefficients computed by Lebreton & Margnac, by Keil and by Bai & Yeung remain finite, whereas those computed by Yu & Ursell and by Kim tend to infinity as the frequency tends to zero. Ursell (1974) showed analytically that the heave added mass in water of finite depth is finite. Chung, Bomze & Coleman (1974) also showed good agreement between their computation and the results obtained by Bai & Yeung. More recently, Kim (1975) was able to compute added-mass coefficients which agree with the results of Bai & Yeung for small frequencies by taking finer meshes in the computations.

In this paper, a simple proof is given in §3 that the added-mass coefficients of a semi-submerged body heaving in water of finite depth are finite: the proof given in the present paper is simpler than that given by Ursell (1974). This result for finite depth is contrary to the result of Ursell (1949) for water of infinite depth in the limiting case of zero frequency. We also present a new formulation for the zero-frequency limit by using a perturbation expansion for a small wavenumber. The limiting case of infinite frequency is also considered here. Both limiting cases are solved numerically by the finite-element method. As the basis of the numerical method, we used the dual extremum principles, which give upper and lower bounds on the added-mass coefficients in the limiting problems. For completeness, results for the problem with arbitrary frequency are also presented. The added-mass coefficients computed from two different formulations are compared. Numerical tests of the upper and lower bounds are also presented.

The added mass for the limiting frequencies can be computed by other numerical methods such as the method of singularity distributions, and finite-difference method, etc. However, for these methods there is no general criterion for the estimation of the accuracy of the numerical results. In most numerical methods, one has to make several calculations to obtain an acceptable approximation to the solution. In contrast, the dual extremum principles provide a pair of numerical values which are, respectively, upper and lower bounds of the exact solution. Therefore, the biggest advantage of the present method is that one obtains an absolute measure of the accuracy of each numerical result. The present results can also serve to check the accuracy of approximate solutions obtained by other methods.

2. Formulation of the problem

A right-handed rectangular co-ordinate system is used with the y axis directed oppositely to the force of gravity and the x axis in the undisturbed free surface. It is assumed that the fluid is inviscid and incompressible and that the flow is irrotational; hence there exists a velocity potential. Furthermore, surface tension is neglected and simple harmonic motions are assumed.

The two-dimensional oscillatory flow is described by the velocity potential

$$\Phi(x, y, t) = \mathrm{Re}\{\phi(x, y)\, e^{-i\sigma t}\}, \tag{2.1}$$

where σ is the frequency and $\phi(x, y)$ is the complex spatial velocity potential, which must satisfy

$$\nabla^2 \phi(x, y) = 0 \tag{2.2}$$

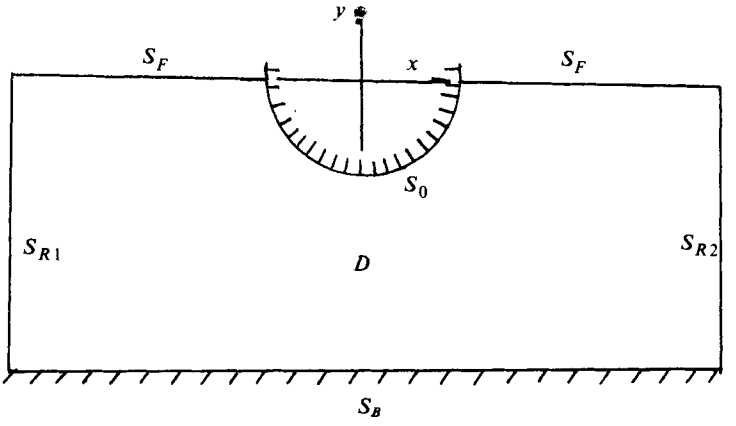

FIGURE 1. Domain of definition and boundary configuration.

in the fluid domain D. The boundary of the fluid domain D consists of the body boundary, the free surface, both infinities and the bottom, which are denoted, respectively, by S_0, S_F, S_{R1}, S_{R2} and S_B, as shown in figure 1. The body is assumed to undergo a small forced vertical displacement

$$Y(t) = (Y_0/\sigma)\sin\sigma t, \tag{2.3}$$

where Y_0 is the amplitude of heave velocity. If Y_0 is taken as unity, the boundary condition on the cylinder is

$$\phi_n = V_n = n_2, \tag{2.4}$$

where $\mathbf{n} = (n_1, n_2)$ is the outward unit normal vector.

Since the motions are small, it can be assumed that the resulting free-surface disturbances are also small, so that the linearized free-surface boundary condition can be applied:

$$\phi_y - \nu_0\phi = 0 \quad \text{on} \quad S_F, \tag{2.5}$$

where

$$\nu_0 = \sigma^2/g. \tag{2.6}$$

The bottom boundary condition for finite depth h is

$$\phi_n = 0 \quad \text{on} \quad S_B. \tag{2.7}$$

The radiation condition requires that the disturbances at the infinities are outgoing waves; hence

$$\lim_{x\to\pm\infty}(\phi_x \mp ik\phi) = 0, \tag{2.8}$$

where k is the wavenumber and is determined by

$$\nu_0 = k\tanh kh. \tag{2.9}$$

Then the added-mass coefficient μ and damping coefficient λ are defined by the integral

$$\mu + i\lambda/\sigma = \rho\int_{S_0}\phi\phi_n\,dS, \tag{2.10}$$

where ρ is the density of water and $\phi = \phi_1 + i\phi_2$ is the potential for unit heave velocity. The above problem was solved by Bai & Yeung (1974) using the localized-finite-element

method based on a variational principle. Two functionals were constructed in their paper.

3. Proof of the boundedness of the added mass

It is proved here that the added mass is bounded for all frequencies in water of finite depth. Let us consider a *thin* wedge described by

$$x = \pm f(y) \tag{3.1}$$

undergoing the heave motion given in (2.3). The linearized body boundary condition can be expressed along the centre-line ($x = 0$) as

$$\phi_n = V_n = df(y)/dy, \tag{3.2}$$

where df/dy is also assumed to be small. Here the amplitude of the heave velocity is assumed to be unity. Owing to symmetry, only half of the fluid domain ($x \geqslant 0$) is considered. Then the eigenfunctions of this problem are

$$\{\exp(ikx)\cosh k(y+h), \exp(-m_i x)\cos m_i(y+h)\}, \tag{3.3}$$

where k is the wavenumber defined earlier and m_i ($i = 1, 2, \ldots$) is defined by

$$-\nu_0 = m_i \tan m_i h. \tag{3.4}$$

Then the original problem of the heaving wedge is reduced to the well-known wave-maker problem treated in detail by Wehausen (1967). Following Wehausen closely, the potential Φ can be expressed as

$$\Phi = \frac{a_0}{k}\cosh k(y+h)\sin(kx-\sigma t) - \sum_{i=1}^{\infty}{}^{*}\frac{a_i}{m_i}\exp(-m_i x)\cos m_i(y+h)\cos\sigma t, \tag{3.5}$$

where the coefficients a_0 and a_i ($i = 1, 2, \ldots$) are defined as

$$\left.\begin{aligned} a_0 &= \frac{4k}{\sinh 2kh + 2kh}\int_{-h}^{0} -V_n \cosh k(y+h)\,dy, \\ a_i &= \frac{4m_i}{\sin 2m_i h + 2m_i h}\int_{-h}^{0} -V_n \cos m_i(y+h)\,dy. \end{aligned}\right\} \tag{3.6}$$

The added mass of the heaving wedge can be expressed as

$$\mu = \frac{\rho}{2}\sum_{i=1}^{\infty}\frac{a_i^2}{m_i^2}[m_i h + \tfrac{1}{2}\sin 2m_i h]. \tag{3.7}$$

Substitution of (3.6) in (3.7) gives

$$\begin{aligned} \mu &= \frac{\rho}{2}\sum_{i=1}^{\infty}\left\{\frac{m_i h + \frac{1}{2}\sin 2m_i h}{m_i^2}\left[\frac{4m_i\int_{-h}^{0} -V_n\cos m_i(y+h)\,dy}{\sin 2m_i h + 2m_i h}\right]^2\right\} \\ &= 4\rho\sum_{i=1}^{\infty}\frac{\left[\int_{-h}^{0} V_n\cos m_i(y+h)\,dy\right]^2}{\sin 2m_i h + 2m_i h} \\ &= 4\rho\left\{\sum_{i=1}^{L}\frac{\left[\int_{-h}^{0} V_n\cos m_i(y+h)\,dy\right]^2}{\sin 2m_i h + 2m_i h} + \sum_{L+1}^{\infty}\frac{\left[\int_{-h}^{0} V_n\cos m_i(y+h)\,dy\right]^2}{\sin 2m_i h + 2m_i h}\right\}, \end{aligned} \tag{3.8}$$

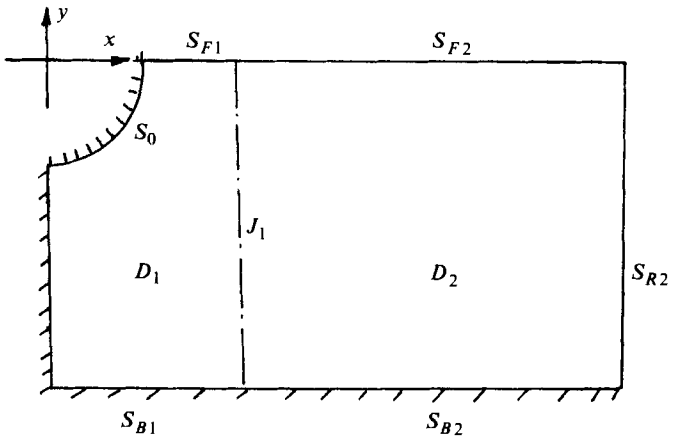

FIGURE 2. Subdomains of fluid domain separated by J_1.

where L is a large integer. By noting the relations

$$\tfrac{1}{2}(2j-1)\pi < m_j h \leqslant j\pi \quad \text{for} \quad j = 1, 2, \ldots, \tag{3.9}$$

the integral in the second term in (3.8) becomes

$$\int_{-h}^{0} V_n \cos m_i(y+h)\, dy = O(1/m_i) \quad \text{as} \quad m_i \to \infty. \tag{3.10}$$

Equation (3.10) is equivalent to the Riemann–Lebesgue lemma. By using (3.10), (3.8) reduces to

$$\mu = 4\rho \sum_{1}^{L} \frac{\left[\int_{-h}^{0} V_n \cos m_i(y+h)\, dy\right]^2}{2m_i h + \sin 2m_i h} + \sum_{L+1}^{\infty} O\left(\frac{1}{m_i^3}\right). \tag{3.11}$$

It follows from (3.11) that the added mass μ is bounded for finite water depth h. It is of interest to note that this proof fails when the water depth h tends to infinity, as expected from the well-known result of Ursell (1949).

The above proof can be generalized to any body geometry by using the eigenfunctions along an artificial boundary J_1 which separates the fluid domain into two subdomains as shown in figure 2. We denote the subdomain which contains the body boundary by D_1 and the other semi-infinite subdomain by D_2. Besides the common boundary J_1, the boundary consists of the body, the free surface and the bottom, respectively denoted by S_0, S_{F1} and S_{B1} for the subdomain D_1; similarly, the free surface, the bottom and the boundary at infinity in D_2 are denoted, respectively, by S_{F2}, S_{B2} and S_{R2}. Then the added mass is expressed by

$$\mu = \rho \int_{S_0} \phi_1 V_n\, dS = \rho \iint_{D_1} (\nabla\phi_1)^2\, dx\, dy - \rho\nu_0 \int_{S_{F1}} \phi_1^2\, dS - \rho \int_{J_1} \phi_1 \phi_{1n}\, dS, \tag{3.12}$$

where $\phi = \phi_1 + i\phi_2$ and V_n is assumed real. In (3.12) the first two integrals are bounded since $\nabla\phi_1$ and ϕ_1 are bounded everywhere in the fluid domain D_1, and the last integral is also finite as a consequence of the proof given earlier. Therefore the added mass is proved to be finite.

4. The reduction of the problem for the limiting cases

The potential ϕ is indeterminate when the frequency is zero owing to an additive constant which arises in the formulation given in §2. The result at zero frequency can be obtained only as a limit of the results for frequency approaching zero. Therefore we reformulate the oscillatory-cylinder problem for the limiting case of zero frequency by using the method of perturbation expansions. Throughout this section, the cylinder is assumed to be symmetric with respect to the y axis. Henceforth only half of the fluid domain is considered.

4.1. *Zero-frequency problem*†

It is convenient to introduce a non-dimensional wavenumber as the perturbation parameter:

$$\epsilon = kh. \tag{4.1}$$

Let a be the half-beam of the rigid cylinder, i.e. the x co-ordinate of the intersection point of the body and the free surface. Owing to symmetry, only half of the fluid domain ($x \geqslant 0$) is considered. It is assumed that the depth of water h is of the same order as a, so that

$$a/h = O(1). \tag{4.2}$$

The following asymptotic expression for the velocity potential will be used:

$$\phi = \phi^{(0)} + \epsilon\phi^{(1)} + \epsilon^2\phi^{(2)} + \dots. \tag{4.3}$$

The existence (as well as the uniqueness) of this asymptotic expansion was proved by Ogilvie (1960). Consequently the normal velocity on the cylinder V_n can be expressed as

$$V_n = V_n^{(0)} + \epsilon V_n^{(1)}, \tag{4.4}$$

where V_n is assumed real.

By use of (2.9) and (4.1), the free-surface condition (2.5) reduces to

$$\phi_y - (\epsilon/h)\tan(\epsilon)\,\phi = 0, \tag{4.5}$$

and by use of (4.1), the radiation condition (2.8) becomes

$$\phi_x = i\epsilon\phi/h \quad \text{as} \quad x \to \infty. \tag{4.6}$$

By expanding (4.5) in a Taylor series, we obtain

$$\phi_y = (\epsilon^2 - \tfrac{1}{3}\epsilon^4)\,\phi/h + O(\epsilon^6). \tag{4.7}$$

By substituting (4.3) and (4.4) in (2.2), (2.4), (2.7), (4.6) and (4.7) and collecting terms of the same order in ϵ, we obtain, referring to figure 1, the following problems.

(i) The zero-order problem:

$$\nabla^2\phi^{(0)} = 0 \quad \text{in} \quad D, \tag{4.8a}$$

$$\phi_y^{(0)} = 0 \quad \text{on} \quad S_F, \quad \phi_n^{(0)} = V_n^{(0)} \quad \text{on} \quad S_0, \tag{4.8b,c}$$

$$\phi_x^{(0)} = 0 \quad \text{on} \quad S_{R2}, \quad \phi_n^{(0)} = 0 \quad \text{on} \quad S_B, \tag{4.8d,e}$$

$$\phi_n^{(0)} = 0 \quad \text{on} \quad x = 0. \tag{4.8f}$$

† Professor J. N. Newman (private communication, 1975) has formulated this problem independently by a method different from the present one.

(ii) The first-order problem:

$$\nabla^2\phi^{(1)} = 0 \quad \text{in} \quad D, \tag{4.9a}$$

$$\phi_y^{(1)} = 0 \quad \text{on} \quad S_F, \quad \phi_n^{(1)} = V_n^{(1)} \quad \text{on} \quad S_0, \tag{4.9b,c}$$

$$\phi_x^{(1)} = i\phi^{(0)}/h \quad \text{on} \quad S_{R2}, \quad \phi_n^{(1)} = 0 \quad \text{on} \quad S_B, \tag{4.9d,e}$$

$$\phi_n^{(1)} = 0 \quad \text{on} \quad x = 0. \tag{4.9f}$$

(iii) The jth-order problem (for $j = 2, 3$)†:

$$\nabla^2\phi^{(j)} = 0 \quad \text{in} \quad D, \tag{4.10a}$$

$$\phi_y^{(j)} = \phi^{(j-2)}/h \quad \text{on} \quad S_F, \quad \phi_n^{(j)} = 0 \quad \text{on} \quad S_0, \tag{4.10b,c}$$

$$\phi_x^{(j)} = i\phi^{(j-1)}/h \quad \text{on} \quad S_{R2}, \quad \phi_n^{(j)} = 0 \quad \text{on} \quad S_B, \tag{4.10d,e}$$

$$\phi_n^{(j)} = 0 \quad \text{on} \quad x = 0. \tag{4.10f}$$

A fundamental property of a harmonic function is that

$$\oint \phi_n^{(j)}\, dS = 0 \quad (j = 0, 1, 2, \ldots) \tag{4.11}$$

for any simply connected closed contour in D. By applying (4.11) to each of the boundary-value problems (4.8), (4.9) and (4.10) we obtain

$$V_n^{(0)} = 0 \quad \text{on} \quad S_0, \tag{4.12}$$

$$\int_{S_0} V_n^{(1)}\, dS + \frac{i}{h}\int_{S_{R2}} \phi^{(0)} dS = 0 \tag{4.13}$$

and

$$\int_{S_F} \phi^{(j-2)} dS + i\int_{S_{R2}} \phi^{(j-1)} dS = 0 \quad (j = 2, 3). \tag{4.14}$$

From (4.12) we obtain

$$\phi^{(0)} = C^{(0)}, \tag{4.15}$$

where the constant $C^{(0)}$ is to be determined. From (4.13) and (4.15) we obtain

$$Q + iC^{(0)} = 0, \tag{4.16}$$

where Q is the flux through the body boundary:

$$Q = \int_{S_0} V_n^{(1)} dS. \tag{4.17}$$

Then the constant $C^{(0)}$ in (4.15) is determined as

$$\phi^{(0)} = C^{(0)} = iQ. \tag{4.18}$$

From (4.18), it follows that (4.9d) reduces to

$$\phi_x^{(1)} = i\phi^{(0)}/h = -Q/h \quad \text{on} \quad S_{R2}, \tag{4.19}$$

† The boundary condition (4.10b) can be expressed in an infinite series for more general cases i.e. $j \geqslant 0$, as follows:

$$\phi_y^{(j)} = \frac{1}{h}\phi^{(j-2)} - \frac{1}{3}\frac{1}{h}\phi^{(j-4)} + \frac{2}{15}\frac{1}{h}\phi^{(j-6)} + \ldots,$$

where a ϕ with a negative superscript is understood to be zero.

and hence we find that $\phi^{(1)}$ should behave like

$$\phi^{(1)} = (-Q/h)\,x + C^{(1)}, \tag{4.20}$$

where $C^{(1)}$ is a constant. By using (4.18) and (4.20) it follows from (4.14) with $j = 2$ that

$$i(x-a)\,Q/h + i(C^{(1)} - Qx/h) = 0 \quad \text{on} \quad S_{R2} \tag{4.21}$$

and hence the constant $C^{(1)}$ is

$$C^{(1)} = Qa/h. \tag{4.22}$$

From (4.20) and (4.22), the infinity condition (4.9d) becomes

$$\phi^{(1)} = (-Q/h)\,(x-a) \quad \text{on} \quad S_{R2}. \tag{4.23}$$

It is easily shown that if boundary condition (4.9d) is replaced by (4.23) then a unique solution can be obtained to (4.9).

By using the same procedure we can determine successively the constants $C^{(j)}$ ($j = 2, 3$), defined by

$$\phi^{(j)} = -\frac{1}{h}\int_a^x \phi^{(j-2)}(\xi, 0)\,d\xi + C^{(j)}, \tag{4.24}$$

by applying the flux relation given by (4.14). For example, for large x

$$\phi^{(2)} = -i\,[Q(x-a)^2/2h^2] + C^{(2)}, \tag{4.25}$$

where $C^{(2)}$ is determined from

$$C^{(2)} = \lim_{x\to\infty}\left\{\frac{i}{h}\int_a^x \phi^{(1)}(\xi, 0)\,d\xi + \frac{iQ}{2h^2}(x-a)^2\right\}. \tag{4.26}$$

Since in the present work we are only interested in examining problems up to the first order, we do not need to determine the constants defined in (4.24). It should be noted that in the jth-order problem for $j = 0, 1, 2, \ldots$, the solution $\phi^{(j)}$ is real when j is odd and imaginary when j is even. This relation will be used below.

When we consider the potential ϕ in (4.3), retaining only terms up to order ϵ, we have

$$\phi = \epsilon[iQ/\epsilon + \phi^{(1)}] + O(\epsilon^2). \tag{4.27}$$

For a heave velocity of unit amplitude, i.e.

$$V_n = \epsilon V_n^{(1)} = n_2, \tag{4.28}$$

the potential ϕ in (4.27) becomes

$$\phi = [ia/\epsilon + \phi^{(1)}] + O(\epsilon). \tag{4.27'}$$

Then the added-mass and damping coefficients defined in (2.10) may be expressed as

$$\mu + i\frac{\lambda}{\sigma} = \rho\int_{S_0}\left(\frac{ia}{\epsilon} + \phi^{(1)}\right) n_2\,dS + O(\epsilon). \tag{4.29}$$

More specifically, by using the fact that the even-order potential is imaginary as mentioned earlier, (4.29) reduces to

$$\mu = \rho\int_{S_0}\phi^{(1)} n_2\,dS + O(\epsilon^2), \tag{4.30a}$$

$$\lambda = \rho\sigma a^2/\epsilon + O(\epsilon). \tag{4.30b}$$

By using the relation

$$\sigma^2 h/g = \epsilon \tanh \epsilon = \epsilon^2 + O(\epsilon^4) \quad \text{for small } \epsilon, \tag{4.31}$$

we obtain from (4.30*b*)

$$\lambda = \rho a^2 (g/h)^{\frac{1}{2}} + O(\epsilon). \tag{4.32}$$

The asymptotic formula (4.32) shows that the damping coefficient λ is a function of only the half-beam a and the water depth h and that it is independent of the shape of the submerged part of the body.

It is also of interest to note that for higher-order problems the added mass can be expressed as

$$\mu = \mu^{(1)} + \epsilon^2 \mu^{(3)} + O(\epsilon^4), \tag{4.33}$$

where

$$\mu^{(j)} = \rho \int_{S_0} \phi^{(j)} n_2 \, dS \quad (j = 1, 3, 5, \ldots). \tag{4.34}$$

Then $\mu^{(3)}$ becomes the slope of the added-mass curve with respect to the non-dimensional wavenumber $\nu_0 a$, which behaves like $\epsilon^2 a/h$ for small σ.

4.2. *Infinite-frequency case*

The opposite limiting case, when the frequency tends to infinity, can be treated in a straightforward manner. By taking the limit as the frequency goes to infinity, (2.2), (2.4), (2.5), (2.7) and (2.8) are reduced to

$$\nabla^2 \phi = 0 \quad \text{in} \quad D, \tag{4.35a}$$

$$\phi_n = n_2 \quad \text{on} \quad S_0, \quad \phi = 0 \quad \text{on} \quad S_F, \tag{4.35b,c}$$

$$\phi_n = 0 \quad \text{on} \quad S_B, \quad x = 0, \tag{4.35d,e}$$

$$\phi = 0 \quad \text{on} \quad S_{R2}. \tag{4.35f}$$

The solution of (4.35) can be determined uniquely. Here it should be pointed out that a systematic expansion procedure, in the manner of §4.1 for the low-frequency case, is not possible. This high-frequency case was treated by Ursell (1953) for a circular cylinder in water of infinite depth.

5. Dual extremum principles

In this section we discuss the upper and lower bounds of the added mass for both of the limiting cases: zero and infinite frequency. The theory of the calculus of variations shows that the solution of certain types of problem is characterized by both a maximum principle and a (different but related) minimum principle, referred to as the dual extremum principles. These principles are also known as the complementary variational principle or the upper and lower bounding principles. Two of the most familiar pairs of dual extremum principles are the potential- and complementary-energy theorems characterizing equilibrium in classical elasticity and the upper- and lower-bound principles associated with the Dirichlet problem of potential theory. We shall follow the latter in this paper. However, one can find a very extensive and systematic derivation of the dual extremum principles in a unified account of a diverse range of problems by Noble & Sewell (1972).

Miles (1971) showed that Schwinger's variational method can be used to form complementary variational principles which give upper- and lower-bound approxima-

tions to the solution of the problem of surface waves scattering from a circular dock in water of finite depth. Schwinger's method is difficult to apply to non-rectangular geometries, since this method requires a set of eigenfunctions in the subdomains of the fluid; this approach is closely related to the well-known Ritz method.

In the present paper the added masses for the limiting cases are computed by the finite-element method, which does not require the set of known eigenfunctions of the problem. In this approach a set of piecewise-polynomial trial functions is used in each subdivided finite element.

Since the following specific classical dual extremum principles are also discussed in some detail by Courant & Hilbert (1953, pp. 240–242) and Arthurs (1970), we only give a brief description here. Let us first summarize the first-order problem formulated in §4.1. This problem is rewritten, after dropping the superscript (1) on ϕ, as

$$\nabla^2\phi = 0 \quad \text{in} \quad D, \tag{5.1a}$$

$$\phi_y = 0 \quad \text{on} \quad S_F, \quad \phi_n = n_2 \quad \text{on} \quad S_0, \tag{5.1b,c}$$

$$\phi = -a\,(x-a)/h \quad \text{on} \quad S_{R2}, \tag{5.1d}$$

$$\phi_n = 0 \quad \text{on} \quad S_B, \quad x = 0. \tag{5.1e,f}$$

From the classical theory of the calculus of variations, the variational principle equivalent to the zero-frequency problem (5.1) can be expressed as

$$\delta J\{\phi\} = 0 \tag{5.2}$$

with the essential condition (5.1d), where the functional J is defined as

$$J\{\phi\} = -\int\int_D \tfrac{1}{2}(\nabla\phi)^2 + \int_{S_0} n_2\phi\,dS - \int_{S_{R2}} \frac{a}{h}\phi\,dS. \tag{5.3}$$

It should be noted here that the boundary condition (5.1d) is used as a natural condition by making use of the normal velocity computed from (5.1d). Then a sufficient condition for the solution of the functional equation (5.2) to be unique is that the functional (5.3) should satisfy the essential condition (5.1d) at an arbitrary point on S_{R2}, not on the entire boundary S_{R2}.

As an alternative, the zero-frequency problem (5.1) can be described in terms of a stream function ψ:

$$\nabla^2\psi = 0 \quad \text{in} \quad D, \tag{5.4a}$$

$$\psi = 0 \quad \text{on} \quad S_F, \quad \psi = a-x \quad \text{on} \quad S_0, \tag{5.4b,c}$$

$$\psi_n = 0 \quad \text{on} \quad S_{R2}, \quad \psi = a \quad \text{on} \quad S_B, \quad x = 0. \tag{5.4d–f}$$

Here (5.4d) can also be expressed as a Dirichlet-type boundary condition:

$$\psi = (-a/h)\,y \quad \text{on} \quad S_{R2}. \tag{5.4d'}$$

From (5.4) we obtain another variational principle (a complementary or dual variational principle) as follows:

$$\delta K\{\psi\} = 0. \tag{5.5}$$

with the essential boundary conditions (5.4b,c,e,f), where the functional $K\{\psi\}$ is defined as

$$K\{\psi\} = \int\int_D \tfrac{1}{2}(\nabla\psi)^2\,dx\,dy. \tag{5.6}$$

In order to show that the global (not merely local) extrema of the functionals J and K are attained when the exact solutions ϕ_0 and ψ_0 of (5.1) and (5.4) are provided, we introduce a small perturbation as follows:

$$\phi = \phi_0 + \epsilon\tilde{\phi}, \quad \psi = \psi_0 + \epsilon\tilde{\psi}. \tag{5.7a,b}$$

Here ϕ_0 and ψ_0 are the exact solutions, $\tilde{\phi}$ and $\tilde{\psi}$ are arbitrary functions of x and y, satisfying proper essential boundary conditions, and ϵ is a small parameter. By substituting (5.7a) into (5.3) and (5.7b) into (5.6), we obtain

$$J\{\phi_0+\epsilon\tilde{\phi}\} = J_0 - \epsilon\left[\iint_D (-\nabla^2\phi_0)\,\tilde{\phi}\,dx\,dy + \int_{S_0}(\phi_{0n}-n_2)\,\tilde{\phi}\,dS \right.$$
$$\left. \int_{S_F+S_B+y} \phi_{0n}\tilde{\phi}\,dS + \int_{S_{R2}}\left(\phi_{0n}+\frac{a}{h}\right)\tilde{\phi}\,dS\right] - \epsilon^2\left[\iint_D \tfrac{1}{2}(\nabla\tilde{\phi})^2\,dx\,dy\right], \tag{5.8}$$

$$K\{\psi_0+\epsilon\tilde{\psi}\} = K_0 + \epsilon\left[\iint_D (-\nabla^2\psi_0)\,\tilde{\psi}\,dx\,dy + \oint \psi_{0n}\tilde{\psi}\,dS\right] + \epsilon^2\left[\iint_D \tfrac{1}{2}(\nabla\tilde{\psi})^2\,dx\,dy\right], \tag{5.9}$$

where

$$J_0 = -\frac{1}{2}\iint_D (\nabla\phi_0)^2\,dx\,dy + \int_{S_0} n_2\phi_0\,dS - \int_{S_{R2}}\frac{a}{h}\phi_0\,dS, \tag{5.10}$$

$$K_0 = \frac{1}{2}\iint_D (\nabla\psi_0)^2\,dx\,dy. \tag{5.11}$$

In (5.8) and (5.9), we assume that the boundary conditions, the natural and essential conditions, are properly taken into account. Since the velocity fields computed from either the potential or the stream function are the same, we have

$$\iint_D (\nabla\phi)^2\,dx\,dy = \iint_D (\nabla\psi)^2\,dx\,dy. \tag{5.12}$$

By Green's theorem, (5.12) reduces to a line integral along the closed boundary of D:

$$\oint \phi_n\phi\,dS = \oint \psi_n\psi\,dS. \tag{5.13}$$

From (5.10)–(5.13), we obtain

$$J_0 = K_0. \tag{5.14}$$

From (5.8), (5.9) and (5.14), we obtain the following useful inequalities:

$$J\{\phi\} \leqslant J_0 = K_0 \leqslant K\{\psi\}. \tag{5.15}$$

The equalities hold only when ϕ and ψ are the exact solutions.

It is of interest to note that by using Green's theorem J_0 can be further reduced to

$$J_0 = \frac{1}{2}\int_{S_0}\phi_0 n_2\,dS + I_0, \tag{5.16}$$

where

$$I_0 = \int_{S_{R2}} \tfrac{1}{2}\phi_{0x}\phi_0\,dS = \frac{a^2}{2h}(x-a) \tag{5.17}$$

for large x. Here the boundary condition (5.1d) was used in (5.17). On subtracting (5.17) from (5.15) and multiplying by 2ρ, inequalities (5.15) reduce to

$$2\rho[J\{\phi\} - (a^2/2h)(x-a)] \leqslant \mu \leqslant 2\rho[K(\psi) - (a^2/2h)(x-a)] \tag{5.18}$$

for large x.

By a similar procedure, we can describe the infinite-frequency forms of (4.35) by introducing the stream function ψ as follows:

$$\nabla^2\psi = 0 \quad \text{in} \quad D, \tag{5.19a}$$

$$\psi_n = 0 \quad \text{on} \quad S_F, \quad \psi = a - x \quad \text{on} \quad S_0, \tag{5.19b,c}$$

$$\psi = a \quad \text{on} \quad S_B, \quad x = 0, \tag{5.19d,e}$$

$$\psi_n = 0 \quad \text{on} \quad S_{R2}. \tag{5.19f}$$

Then we obtain the following dual extremum principles from (4.35) and (5.19):

$$\delta J\{\phi\} = 0 \tag{5.20}$$

with the essential condition (4.35c, f) and

$$\delta K\{\psi\} = 0 \tag{5.21}$$

with the essential conditions (5.19c–e). Here J and K are defined as

$$J\{\phi\} = -\iint_D \tfrac{1}{2}(\nabla\phi)^2\,dx\,dy + \int_{S_0} n_2\phi\,dS \tag{5.22}$$

and

$$K\{\psi\} = \iint_D \tfrac{1}{2}(\nabla\psi)^2\,dx\,dy. \tag{5.23}$$

By a procedure similar to that used for the zero-frequency case, it may be shown that the upper and lower bounds on the added mass μ at infinite frequency are given by

$$2\rho J\{\phi\} \leqslant \mu \leqslant 2\rho K\{\psi\}. \tag{5.24}$$

It is of interest to note that (5.18) and (5.24) can be respectively interpreted as the maximum principle of the added mass with the functional J and the minimum principle with the complementary functional K. The minimum principle of the added mass was discussed by Garabedian & Spencer (1952) in connexion with cavity flow problems.

6. Numerical results and discussion

The numerical details of the finite-element method can be found in Bai (1972, 1975a, b). The infinity boundary condition was applied at a finite but sufficient distance from the body. One can easily show, by using eigenfunction expansions, that the error due to the truncation of the original infinite boundary is negligibly small. Throughout the present numerical results, the last significant digit was rounded down for the lower bound and rounded up for the upper bound.

In this section we present the results obtained by the two different methods: the dual extremum principles applied to the limiting cases treated in §§ 4 and 5, and the localized finite-element method applied to the general frequency range as described in Bai & Yeung (1974). The hydrodynamic coefficients are non-dimensionalized by making use of the submerged area S as follows:

$$\hat{\mu} = \mu/\rho S, \quad \hat{\lambda} = \lambda/\sigma\rho S. \tag{6.1}$$

Here it should be remembered that S is half of the total submerged area since only half of the fluid domain is treated owing to symmetry. We denote the non-dimensional

	$\hat{\mu}_0$		$\hat{\mu}_\infty$	
h/a	Lower bound	Upper bound	Lower bound	Upper bound
1·2	0·9565	0·9577	1·8326	1·8344
1·5	0·6253	0·6263	1·4441	1·4456
2·0	0·4968	0·4976	1·2235	1·2247
2·5	0·4957	0·4967	1·1355	1·1369
3·0	0·5325	0·5326	1·0909	1·0920
4·0	0·6291	0·6370	1·0452	1·0523
5·0	0·7315	0·7438	1·0242	1·0331
6·0	0·8421	0·8512	1·0163	1·0236

TABLE 1. The upper and lower bounds on $\hat{\mu}_0$ and $\hat{\mu}_\infty$ for a circular cylinder of radius x in water of depth h.

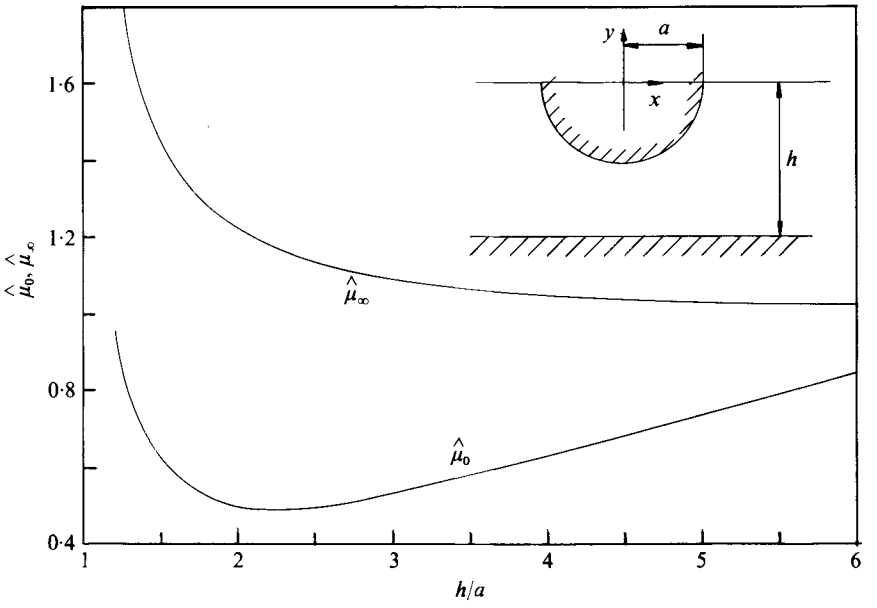

FIGURE 3. The added masses $\hat{\mu}_0$ and $\hat{\mu}_\infty$ of a circular cylinder *vs.* the water depth.

added-mass and damping coefficients for the zero-frequency limiting problem by $\hat{\mu}_0$ and $\hat{\lambda}_0$, those for the infinite-frequency limiting problem by $\hat{\mu}_\infty$ and $\hat{\lambda}_\infty$, and those for the case of general frequency by $\hat{\mu}(\sigma)$ and $\hat{\lambda}(\sigma)$. Then the non-dimensional damping coefficient for the zero-frequency limit can be expressed, from the asymptotic formula (4.32), as

$$\hat{\lambda}_0 = \frac{4}{\pi}(\nu_0 h)^{-\frac{1}{2}} = \frac{4}{\pi}\left(\frac{\nu h}{a}\right)^{-\frac{1}{2}} \tag{6.2a}$$

for a circular cylinder and as

$$\hat{\lambda}_0 = \frac{a}{b}(\nu_0 h)^{-\frac{1}{2}} = \frac{a}{b}\left(\frac{\nu h}{a}\right)^{-\frac{1}{2}} \tag{6.2b}$$

for a rectangular cylinder with draft b. Here the non-dimensional wavenumber ν is defined by

$$\nu = \nu_0 a = \sigma^2 a/g. \tag{6.3}$$

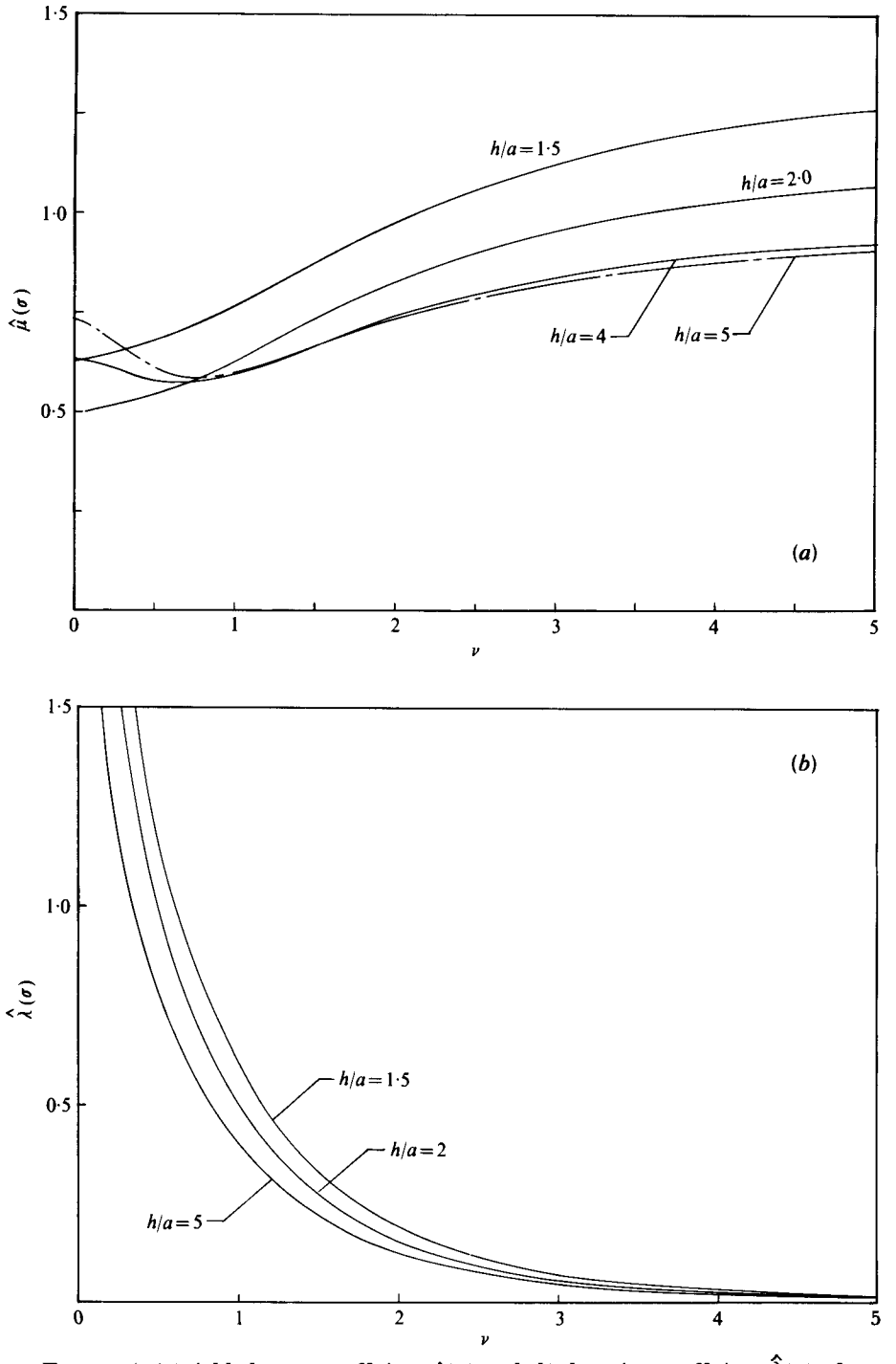

FIGURE 4. (*a*) Added-mass coefficient $\hat{\mu}(\sigma)$ and (*b*) damping coefficient $\hat{\lambda}(\sigma)$ of a circular cylinder *vs.* ν.

ν	$h/a = 1{\cdot}5$	$h/a = 2$	$h/a = 5$
0·001	0·62535	0·49691	0·73176
0·005	0·62572	0·49718	0·73114
0·01	0·62616	0·49749	0·73036
0·05	0·62974	0·50015	0·72358
0·1	0·63444	0·50372	0·71381
0·2	0·64450	0·51165	0·68991
0·4	0·66764	0·53138	0·63307

TABLE 2. The added mass $\hat{\mu}(\sigma)$ of a circular cylinder for small ν.

	$h/a = 1{\cdot}5$		$h/a = 2$		$h/a = 5$	
ν	$\hat{\lambda}(\sigma)$	$\hat{\lambda}_0$	$\hat{\lambda}(\sigma)$	$\hat{\lambda}_0$	$\hat{\lambda}(\sigma)$	$\hat{\lambda}_0$
0·0001	103·9751	103·9596	90·0320	90·0316	56·9383	56·9410
0·001	32·8629	32·8749	28·4592	28·4705	18·0081	18·0063
0·005	14·6733	14·7021	12·7064	12·7324	8·0566	8·0527
0·01	10·3543	10·3960	8·9669	9·0032	5·6992	5·6941
0·05	4·5578	4·6492	3·9447	4·0263	2·5581	2·5465
0·1	3·1576	3·2875	2·7306	2·8471	1·8171	1·8006
0·2	2·1392	2·3246	1·8459	2·0132	1·2939	1·2732
0·4	1·3769	1·6437	1·1800	1·4235	0·9017	0·9003

TABLE 3. Comparisons of the damping coefficients $\hat{\lambda}(\sigma)$ and $\hat{\lambda}_0$ of a circular cylinder for $h/a = 1{\cdot}5$, 2·0 and 5·0.

6.1. *Circular cylinder*

Added-mass coefficients are presented for the zero- and infinite-frequency limiting cases at eight water depths: $h/a = 1{\cdot}2$, 1·5, 2, 2·5, 3, 4, 5 and 6. The lower and upper bounds on the added mass for the limiting cases are given in table 1. The means of both bounds are also plotted in figure 3, since the lower and upper bounds are very close. The added-mass coefficients $\hat{\mu}_0$ and $\hat{\mu}_\infty$ increase indefinitely as the depth h approaches the draft a. It is also of interest to note that $\hat{\mu}_\infty$ decreases as h increases and approaches unity asymptotically; this is the well-known result for an infinite fluid. However, $\hat{\mu}_0$ has a minimum value at a critical depth h_c, which is approximately $2{\cdot}2a$. The value of $\hat{\mu}_0$ increases monotonically as the depth increases beyond the critical depth.

The added-mass and damping coefficients $\hat{\mu}(\sigma)$ and $\hat{\lambda}(\sigma)$ are shown in figures 4(*a*) and (*b*), respectively, for several different depths: $h/a = 1{\cdot}5$, 2, 4 and 5. Numerical results for $\hat{\mu}(\sigma)$ are given in table 2 for some values of small ν. In figure 4(*a*) the values of $\hat{\mu}_0$ shown in figure 3 were used to continue the $\hat{\mu}(\sigma)$ curve up to $\nu = 0$. Figure 4(*a*) shows that in general the $\hat{\mu}(\sigma)$ curve has non-zero slope at $\nu = 0$, as was discussed at the end of § 4.1. It is of interest to note that the slope of the $\hat{\mu}(\sigma)$ curve at $\nu = 0$ is positive when $h < h_c$ and is negative when $h > h_c$. We also observe that, when $h < h_c$, $\hat{\mu}(\sigma)$ increases from the minimum value of $\hat{\mu}_0$ at $\nu = 0$ and approaches asymptotically the maximum value of $\hat{\mu}_\infty$ as the depth h increases.

The damping coefficients $\hat{\lambda}(\sigma)$ are compared with $\hat{\lambda}_0$ for small ν values in table 3. The values of $\hat{\lambda}_0$ were computed from the asymptotic formula (6.2*a*) and the agreement

No. of elements (no. of nodes)	$\hat{\mu}_0$ Lower bound	$\hat{\mu}_0$ Upper bound	Relative error
3 (18)	0·6349	1·2798	0·34
5 (26)	0·7398	0·9096	0·10
14 (59)	0·7727	0·8521	0·05
92 (319)	0·8061	0·8232	0·01

TABLE 4. Convergence of the upper and lower bounds on $\hat{\mu}_0$ for a rectangular cylinder with $h/b = 2$, $a/b = 1$.

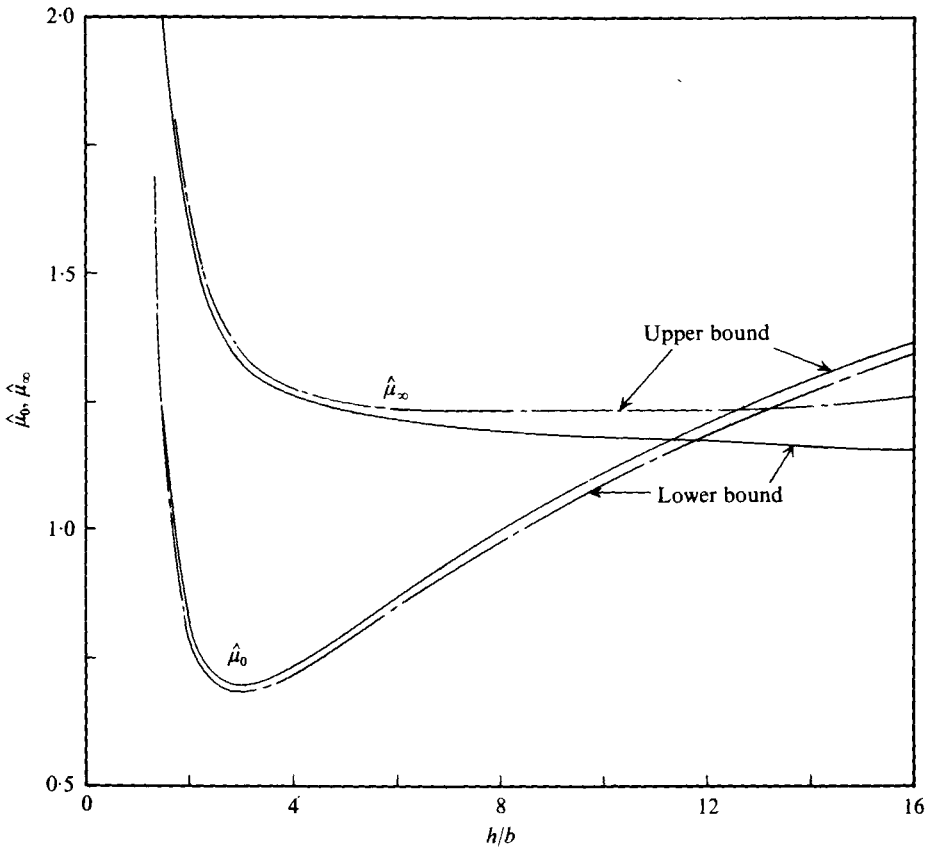

FIGURE 5. Upper and lower bounds on the added-mass coefficients $\hat{\mu}_0$ and $\hat{\mu}_\infty$ of a rectangular cylinder with $a/b = 1$ *vs.* the water depth.

between $\hat{\lambda}(\sigma)$ and $\hat{\lambda}_0$ is excellent for the very small ν. The agreement is still reasonable up to $\nu = 0{\cdot}4$ for $h/a = 5$. In the numerical computations, ten straight-line segments (equally spaced at 9°) are taken along a circle.

	$\hat{\mu}_0$		$\hat{\mu}_\infty$	
h/b	Lower bound	Upper bound	Lower bound	Upper bound
1·1	4·5681	4·7090	5·4820	5·5564
1·2	2·5918	2·6459	3·4666	3·5170
1·5	1·2532	1·2820	2·0969	2·1213
3·0	0·6800	0·6948	1·3343	1·3574
8·0	0·9784	0·9993	1·1943	1·2326
16·0	1·3432	1·3667	1·1550	1·2603

TABLE 5. The lower and upper bounds on $\hat{\mu}_0$ and $\hat{\mu}_\infty$ for a rectangular cylinder with $a/b = 1$ for various depths.

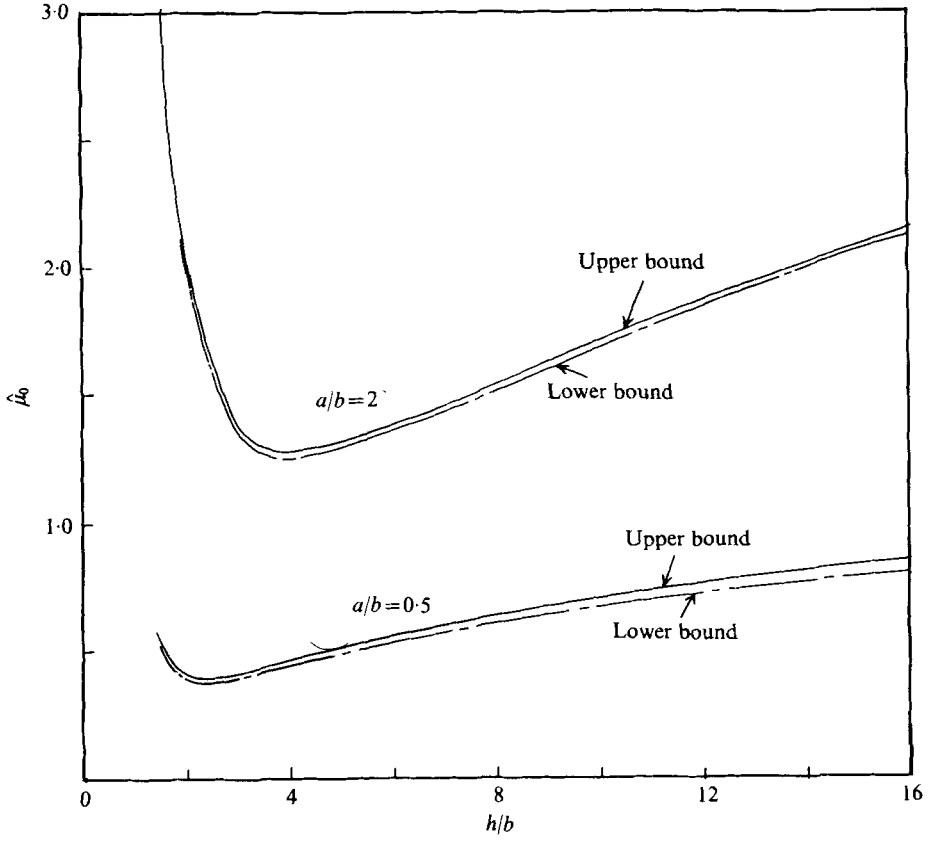

FIGURE 6. Upper and lower bounds on the added-mass coefficients $\hat{\mu}_0$ of rectangular cylinders with $a/b = 0·5$ and $2·0$ *vs.* the water depth.

6.2. *Rectangular cylinders*

We treat here rectangular cylinders with half-beam a and draft (submergence) b in water of depth h. Specifically, three different rectangular sections with $a/b = 0·5$, 1 and 2 are considered for various depths and frequencies.

A numerical experiment was performed to test the convergence of the upper and lower bounds of the added mass $\hat{\mu}_0$ as a function of the number of elements (or nodes)

	$a/b = 0{\cdot}5$		$a/b = 2$	
h/b	Lower bound	Upper bound	Lower bound	Upper bound
1·5	0·5108	0·5240	3·5501	3·7971
2·0	0·3958	0·4088	2·0658	2·1113
3·0	0·3992	0·4151	1·3607	1·3930
8·0	0·6058	0·6423	1·5212	1·5446
16·0	0·8131	0·8662	2·1259	2·1539

TABLE 6. The upper and lower bounds on $\hat{\mu}_0$ for $a/b = 0{\cdot}5$ and 2·0 for various depths.

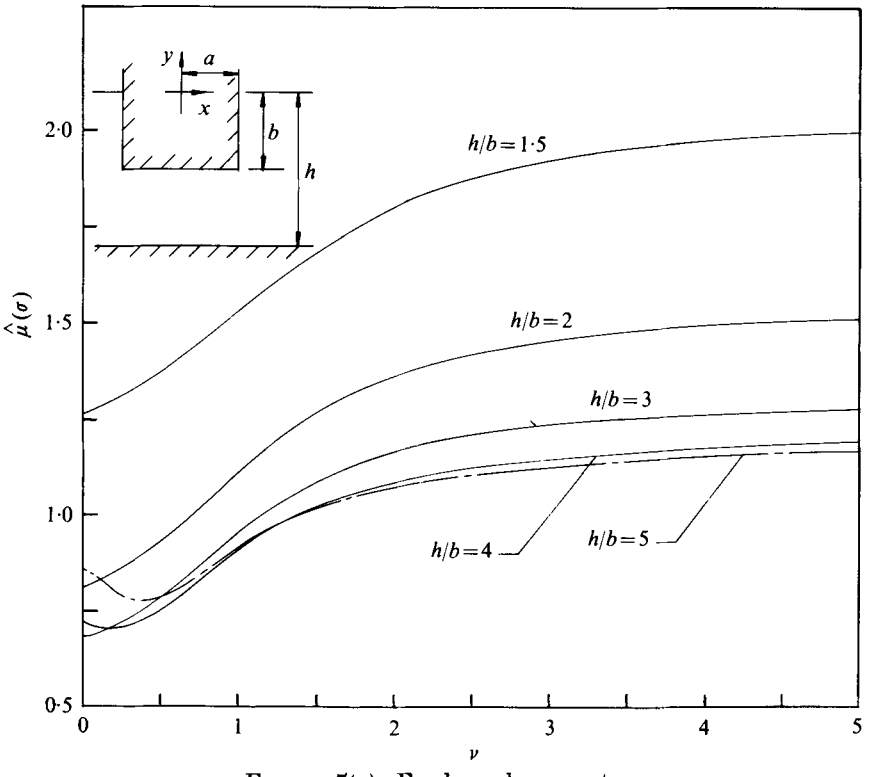

FIGURE 7(*a*). For legend see next page.

for the case $a/b = 1$, $h/b = 2$. The results of the numerical convergence test are given in table 4. The relative errors listed in table 4 are defined as the difference between the two bounds divided by their sum. In all cases, the infinity boundary condition was applied at a sufficiently large distance from the body. It is seen that the relative error decreases very rapidly as the number of nodes increases up to the 5 % error bound. However, a very large number of nodes is required in order to obtain an accuracy of within 1 %.

The upper and lower bounds on $\hat{\mu}_0$ and $\hat{\mu}_\infty$ for $a/b = 1$ were computed for 14 different depths and are shown in figure 5. Some of the numerical results are also given in table 5. The upper and lower bounds on $\hat{\mu}_0$ for $a/b = 0{\cdot}5$ and 2 were computed for

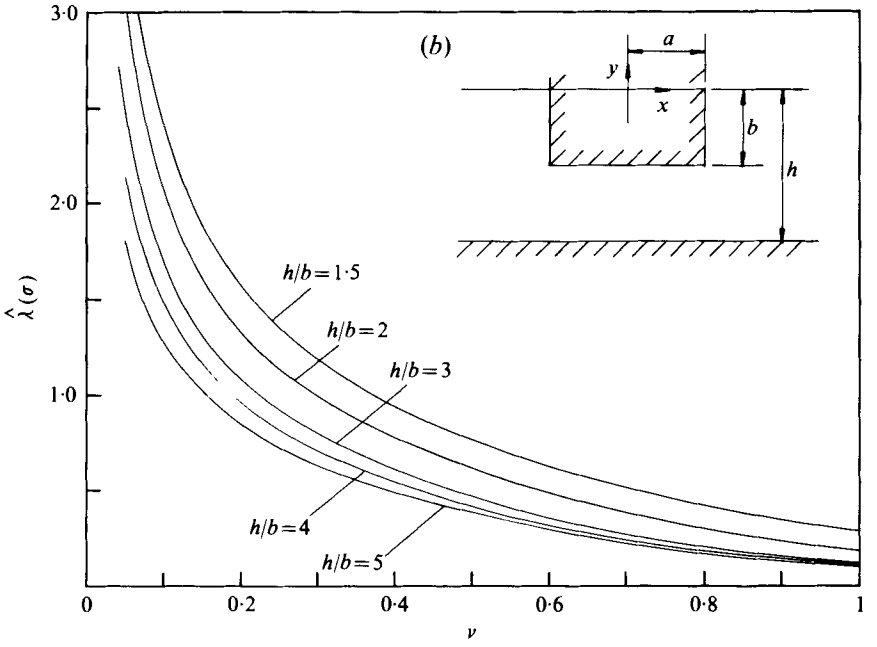

FIGURE 7. (*a*) Added-mass coefficient $\hat{\mu}(\sigma)$ and (*b*) damping coefficient $\hat{\lambda}(\sigma)$ of a rectangular cylinder with $a/b = 1$ *vs.* ν for several water depths.

	$h/b = 3$		$h/b = 6$	
ν	$\hat{\lambda}(\sigma)$	$\hat{\lambda}_0$	$\hat{\lambda}(\sigma)$	$\hat{\lambda}_0$
0·0001	57·6955	57·7350	40·8232	40·8248
0·001	18·2454	18·2574	12·9026	12·9099
0·005	8·1334	8·1650	5·7681	5·7735
0·01	5·7290	5·7735	4·0748	4·0825
0·1	1·6808	1·8257	1·2614	1·2910
0·2	1·0802	1·2910	0·8577	0·9129
0·4	0·6015	0·9129	0·5086	0·6455

TABLE 7. Comparison of $\hat{\lambda}(\sigma)$ and $\hat{\lambda}_0$ for $a/b = 1$ and $h/b = 3$ and 6.

11 different depths and are shown in figure 6. Some of the numerical results are given in table 6. The added mass $\hat{\mu}_0$ has its minimum value at a critical depth h_c and increases monotonically as h increases from h_c; the critical depths h_c are approximately $2{\cdot}3b$ for $a/b = 0{\cdot}5$, $3b$ for $a/b = 1$ and $4b$ for $a/b = 2$ in figures 5 and 6; $\hat{\mu}_0$ also increases indefinitely and rapidly as h approaches the draft b. It is of interest to note that with b fixed the critical depth h_c increases as the beam a increases. However, in figure 5, $\hat{\mu}_\infty$ does not have a minimum value at a finite value of ν and tends to infinity as h approaches b, while as $h \to \infty$ it decreases monotonically and approaches asymptotically a finite value of $\hat{\mu}_\infty = 1{\cdot}1884$, which was obtained by Lewis (1929). Figure 5 also shows that $\hat{\mu}_\infty$ can be approximated by the added mass obtained by Lewis (for the infinite-depth case) to within about 4 % when the depth is larger than 6 times the draft.

The added-mass and damping coefficients $\hat{\mu}(\sigma)$ and $\hat{\lambda}(\sigma)$ are plotted in figures 7 (*a*)

and (*b*) respectively, for the case of $a/b = 1$; computations were performed for values of ν ranging from 0·0001 to 5·0 and five depths: $h/b = 1{\cdot}5$, 2, 3, 4 and 5. In figure 7(*a*), the added-mass curves of $\hat{\mu}(\sigma)$ pass through the corresponding values of $\hat{\mu}_0$ at $\nu = 0$; the curves are very smooth as one should expect. It is of particular interest to note that the $\hat{\mu}(\sigma)$ curves for $h/b = 4$ and 5 have negative slopes at $\nu = 0$, whereas the curves for $h/b = 1{\cdot}5$ and 2 have positive slopes at $\nu = 0$. These results show, as in the case of the circular cylinder, that the slope of the $\hat{\mu}(\sigma)$ curve at $\nu = 0$ is negative when $h > h_c$ and positive when $h < h_c$. Here we can also observe, as in the previous results for the circular cylinder, that $\hat{\mu}(\sigma)$ has its minimum at a finite value of ν, not at $\nu = 0$, when $h > h_c$. However, when $h < h_c$, $\hat{\mu}(\sigma)$ is a monotonically increasing function with a minimum value of $\hat{\mu}_0$ and approaches asymptotically the finite value of $\hat{\mu}_\infty$. The slope of the $\hat{\mu}(\sigma)$ curve for $h/b = 3$ is nearly zero at $\nu = 0$ in figure 7(*a*); this can be interpreted from figure 5, which shows that the critical depth h_c is nearly $3b$.

The damping coefficients $\hat{\lambda}(\sigma)$ shown in figure 7(*b*) are also compared with values of $\hat{\lambda}_0$ computed from the asymptotic formula in (6.2*b*); some of the results are also given in table 7. The comparison shows a good agreement between $\hat{\lambda}(\sigma)$ and $\hat{\lambda}_0$ for small values of ν; as ν increases from 0·01 for the case $h/b = 6$, the results obtained from (6.2*b*) for $\hat{\lambda}_0$ are over-predicted by more than 3 %.

It should be emphasized here that the difference between the upper and lower bounds on the added masses $\hat{\mu}_0$ and $\hat{\mu}_\infty$ presented here can be further reduced simply by taking finer meshes in the domain of the fluid. Since we thought that the error range of the present results is reasonable for engineering purposes, we did not make further attempts to refine our results even though it would be very simple and straightforward to do so.

The author is grateful to Professor T. F. Ogilvie for suggesting this topic, and to Professor J. N. Newman and Professor F. Ursell for their valuable comments during the preparation of this paper. This research was supported by the Numerical Naval Hydrodynamics Program at the David W. Taylor Naval Ship Research and Development Center. A part of this work was done while the author was at the Massachusetts Institute of Technology with the support of the Naval Sea Systems Command's General Hydromechanics Research Program, administered by the David W. Taylor Naval Ship Research and Development Center, Contract N00014-67-A-0204-0081.

Note. After this paper had been completed, recent papers by Fujino (1976) and Sayer & Ursell (1976) came to my attention. Comparisons between their results and the results obtained by the present method are given in my discussions of these two papers. (These discussions will be published with the papers.) A related investigation using the present method will appear in Bai (1977).

REFERENCES

Arthurs, A. M. 1970 *Complementary Variational Principles.* Oxford: Clarendon Press.

Bai, K. J. 1972 A variational method in potential flows with a free surface. Ph.D. dissertation, Department of Naval Architecture, University of California, Berkeley.

Bai, K. J. 1975*a* Diffraction of oblique waves by an infinite cylinder. *J. Fluid Mech.* **68**, 513–535.

BAI, K. J. 1975*b* A localized finite-element method for steady, two-dimensional free-surface flow problems. *1st Int. Conf. Numer. Ship Hydrodyn., David W. Taylor Naval Ship & Dev. Center, Bethesda, Maryland.*

BAI, K. J. 1977 Sway added-mass of cylinders in a canal using dual extremum principles. *J. Ship Res.* **21** (in press).

BAI, K. J. & YEUNG, R. W. 1974 Numerical solutions to free-surface flow problems. *10th Symp. Naval Hydrodyn. Office Naval Res. at M.I.T.*

CHUNG, Y. K., BOMZE, H. & COLEMAN, M. 1974 A discussion of the paper by Bai & Young. *10th Symp. Naval Hydrodyn. Office Naval Res. at M.I.T.*

COURANT, R. & HILBERT, D. 1953 *Methods of Mathematical Physics*, vol. 1. Interscience.

FUJINO, M. 1976 The effect of the restricted waters on the added mass of a rectangular cylinder. *11th Symp. Naval Hydrodyn. Office Naval Res. at University College, London.*

GARABEDIAN, P. R. & SPENCER, D. C. 1952 Extremal methods in cavitational flow. *J. Rat. Mech. Anal.* **1**, 359–409.

KEIL, H. 1974 Die hydrodynamischen Kräfte bei der periodischen Bewegung zweidimensionaler Körper an der Oberfläche fläcker Gewässer. *Inst. Schiffbau, Hamburg, Rep.* no. 305.

KIM, C. H. 1967 Calculation of hydrodynamic forces for cylinders oscillating in shallow water. *Chalmers Univ. Tech., Gothenburg, Sweden, Div. Ship Hydromech. Rep.* no. 36. (See also *J. Ship. Res* **13**, 1969, 137–154.)

KIM, C. H. 1975 Effect of mesh size on the accuracy of finite-water added mass. *Engng Notes, J. Hydronaut.* **9**, 125–126.

LEBRETON, J. C. & MARGNAC, M. A. 1966 Traitement sur ordinateur de quelques problèmes concernant l'action de la houle sur les corps flottants en théorie bidimensionelle. *Bull. Centre Recherches Essais Chatou*, no. 18.

LEWIS, F. M. 1929 The inertia of the water surrounding a vibrating ship. *Trans. Soc. Naval Archit. Mar. Engrs* **37**, 1–20.

MILES, J. W. 1971 A note on variational principles for surface wave scattering. *J. Fluid Mech.* **46**, 141–149.

NOBLE, B. & SEWELL, M. J. 1972 On dual extremum principles in applied mathematics. *J. Inst. Math. Appl.* **9**, 123–193.

OGILVIE, T. F. 1960 Propagation of waves over an obstacle in water of finite depth. *Inst. Engng Res., Univ. California, Berkeley, Rep.* no. 14, ser. 82.

SAYER, P. & URSELL, F. 1976 On the virtual mass, at long wave lengths, of a half-immersed circular cylinder heaving on water of finite depth. *11th Symp. Naval Hydrodyn. Office Naval Res., at University College, London.*

URSELL, F. 1949 On the heaving motion of a circular cylinder in the free surface of a fluid. *Quart. J. Mech. Appl. Math.* **2**, 218–231.

URSELL, F. 1953 Short surface waves due to an oscillating immersed body. *Proc. Roy. Soc.* A **220**, 90–103.

URSELL, F. 1974 Note on the virtual mass and damping coefficients in water of finite depth. *Univ. Manchester, Dept. Math. Rep.*

WEHAUSEN, J. V. 1967 Lecture notes in ship hydrodynamics. *Dept. Naval Archit., Univ. Calif., Berkeley.*

YU, Y. S. & URSELL, F. 1961 Surface waves generated by an oscillating circular cylinder on water of finite depth: theory and experiment. *J. Fluid Mech.* **11**, 529–551.